Eur. Phys. J. D **23**, 343–349 (2003)
DOI: 10.1140/epjd/e2003-00060-6

THE EUROPEAN PHYSICAL JOURNAL D

Magnetism in Rh clusters under hydrostatic deformations

E.O. Berlanga-Ramírez[1,a], F. Aguilera-Granja[1], A. Díaz-Ortiz[2], and A. Vega[3]

[1] Instituto de Física, Universidad Autónoma de San Luis Potosí, 78000 San Luis Potosí, S.L.P., Mexico
[2] Instituto Potosino de Investigación Científica y Tecnológica, Apartado Postal 3-74 Tangamanga, 78231 San Luis Potosí, S.L.P., Mexico
[3] Departamento de Física Teórica, Atómica, Molecular y Nuclear, Universidad de Valladolid, 47011 Valladolid, Spain

Received 5 August 2002 / Received in final form 10 January 2003
Published online 4 March 2003 –

Abstract. The magnetic behavior of rhodium clusters Rh_N ($N = 4$–38) under hydrostatic deformations was investigated. The starting cluster structures were obtained from an evolutionary search algorithm applied to a Gupta potential. The spin-polarized electronic structure and related magnetic properties were calculated using a self-consistent *spd* tight-binding Hamiltonian within the unrestricted Hartree-Fock approximation. The magnetic behavior was analyzed in terms of the interdependence between the geometrical parameters and the electronic structure. Anomalous magnetic effects were found in some cases.

PACS. 36.40.Cg Electronic and magnetic properties of clusters – 61.46.+w Nanoscale materials: clusters, nanoparticles, nanotubes, and nanocrystals

1 Introduction

Cluster physics is instrumental for the understanding of fundamental phenomena in condensed matter physics, such as electronic localization and magnetism. The unique properties exhibited by transition metal (TM) clusters [1–27] as compared with the isolated atom and the bulk can be relevant for the design of high-tech electronic devices. In the case of magnetic nanoparticles, clusters made out of 4*d* and 5*d* TMs deserve special attention because of the magnetic phases that can be stabilized in this low-dimensional regime, despite of the nonmagnetic character of their bulk phase [3,6,28,29]. This behavior was first predicted theoretically in the early 1980s [13] and was later confirmed experimentally for Rh, Ru and Pd, where giant magnetic moments were observed in small clusters [3,6,28,29].

Among 4*d* and 5*d* TMs, clusters containing Rh remain very controversial in literature. These investigations have shown that almost any measurable quantity in clusters depends sensitively on the geometrical structure. Unfortunately, time-of-flight measurements together with pulsed laser evaporation cluster sources can only provide partial information about the size distribution [30,31]. In view of this limitation, theoretical calculations have been performed using both *ab initio* [14,27,32] and semiempirical methods [33,34] in order to elucidate the geometry of the ground state. First-principles density-functional (FP-DFT) calculations, however, are limited to relative small sizes, smaller in general than the ones reported experimentally [3]. On the other hand, semiempirical calculations are less limited in this respect and therefore they are better suited for calculations in the experimental size range.

In a previous work (Ref. [33]), we reported a systematic study of the structural and magnetic properties of Rh_N clusters ($4 \leq N \leq 26$). The ground-state structures together with the low-lying energy isomers were obtained using a Gupta potential together with an evolutionary search algorithm [35,36]. Cluster electronic structure was then calculated using a self-consistent *spd* tight-binding Hamiltonian. Unexpected magnetic behavior of the Rh clusters as a function of interatomic distance and local coordination was found in some cases. A further indication of the complexity of the electronic structure of Rh clusters is the variety of different results obtained, for a given cluster size, with different theoretical approaches. It is not difficult to find in literature different cluster structures or the same structure with different bond-length value [23,33,34] and average magnetic moment per atom [18–22,24–27]. For example, bond-length values between 2.48 and 2.62 Å are reported for tetrahedral Rh_4 clusters [18,23,25,27].

Previously, we obtained magnetic moments in a qualitative good agreement with the experimental values for Rh clusters larger than fifteen atoms, but not for the smaller clusters [33]. The poor agreement between theory and experimental results is common to both FP-DFT and semiempirical approaches. For large clusters, to best of the authors' knowledge, there are no systematic studies available in literature (other than Ref. [33]). Since in all previous studies only the ground-state structure was

[a] e-mail: berlanga@dec1.ifisica.uaslp.mx

considered, in reference [33] we also investigated the effect on the magnetic properties of the coexistence of different structural isomers. The conclusion was that the discrepancy between the magnetic moments obtained in experiment and our calculations at small sizes cannot be attributed to the effect of the coexistence of isomers.

From all the results available for Rh clusters, it is clear that further work is necessary in order to get deeper insight into the complex interdependence between the geometry and the electronic properties. Answering questions like how the magnetic moment of Rh clusters behaves under a particular structural change will help to understand the nature of these systems. In this paper, we study the effect of hydrostatic deformations (*i.e.*, deformations than preserve the point group symmetry while changing the bond length), on the magnetic properties small Rh clusters. To that aim, we used a Hubbard-like Hamiltonian for the $4d$, $5s$ and $5p$ valence electrons within the unrestricted Hartree-Fock approximation [9,10,33]. The model together with some technical details are reviewed in Section 2. The results are presented and discussed in Section 3. The paper finishes with a summary and our conclusions are presented in Section 4.

2 Model

The electronic structure of Rh clusters was determined by solving self-consistently a tight-binding Hamiltonian for the $4d$, $5s$, and $5p$ valence electrons within the unrestricted Hartree-Fock approximation. In a second-quantization notation, the Hamiltonian can be expressed as follows:

$$H = \sum_{i\alpha\sigma} \varepsilon_{i\alpha\sigma}\, \hat{n}_{i\alpha\sigma} + \sum_{\substack{\alpha\beta\sigma \\ i\neq j}} t_{ij}^{\alpha\beta}\, \hat{c}_{i\alpha\sigma}^{+}\, \hat{c}_{j\beta\sigma}, \qquad (1)$$

where $\hat{c}_{i\alpha\sigma}^{+}$ ($\hat{c}_{j\beta\sigma}$) is the creation (annihilation) operator for an electron with spin σ and orbital state α at the atomic site i. The number operator is denoted by $\hat{n}_{i\alpha\sigma}$. The hopping integrals $t_{ij}^{\alpha\beta}$ between orbitals α and β at sites i and j describe the electronic delocalization within the system. For itinerant magnets (TMs), the hopping term in equation (1) is very important. We considered spin-independent hopping integrals up to third-nearest-neighbor distances. The hopping integrals were determined by fitting to the band structure of bulk Rh [37]. However, since interatomic distances in the clusters differ slightly from the bulk, the variation of $t_{ij}^{\alpha\beta}$ with the interatomic distance r_{ij} has been explicitly considered using the typical power law $(r_0/r_{ij})^{l+l'+1}$, where r_0 is the bulk equilibrium distance. The orbital angular momentum of the $(i\alpha\sigma)$ and $(j\beta\sigma)$ states involved in the hopping process are denoted by l, l', respectively. The spin-dependent diagonal terms account for the electron-electron interaction through a correction shift of the energy levels given by

$$\varepsilon_{i\alpha\sigma} = \varepsilon_{i\alpha}^{0} + \frac{z_\sigma}{2} \sum_{\beta} J_{\alpha\beta}\, \mu_{i\beta} + \Omega_{i\alpha}. \qquad (2)$$

Here, $\varepsilon_{i\alpha}^{0}$ are the bare orbital energies of paramagnetic bulk Rh. The second term in the rhs of equation (2) is the correction shift due to the polarization of the electrons at site i ($\mu_{i\beta} = \langle n_{i\beta\uparrow}\rangle - \langle n_{i\beta\downarrow}\rangle$). The exchange integrals are denoted by $J_{\alpha\beta}$, and z_σ is the sign function ($z_\uparrow = 1$, $z_\downarrow = -1$). The exchange integrals involving s and p electrons were neglected taking into account only the integral corresponding to d electrons (J_{dd}). Note that even when the sp exchange integrals are neglected, spin-polarization of the delocalized sp states may exist as a consequence of hybridization with the d states. Usually, J_{dd} is obtained by fitting to the bulk magnetic moment. Due to the fact that Rh metal is paramagnetic, we have taken $J_{dd} = 0.40$ eV so that it reproduces the FP-DFT magnetic moment of icosahedral Rh_{13} [18,38]. Finally, the site- and orbital-dependent (self-consistent) potential $\Omega_{i\alpha}$ assures the local electronic occupation, fixed in our model by interpolating between the isolated atom and the bulk according to the actual local number of neighbors at site i.

The spin-dependent local electronic occupations are self-consistently determined from the local densities of states (DOS)

$$\langle \hat{n}_{i\alpha\sigma}\rangle = \int_{-\infty}^{\varepsilon_{\mathrm{F}}} \mathcal{D}_{i\alpha\sigma}(\varepsilon)\, \mathrm{d}\varepsilon, \qquad (3)$$

which are calculated at each iteration by using the recursion method [39]. In this way, the distribution of the local magnetic moments ($\mu_i = \sum_\alpha \mu_{i\alpha}$) and the average magnetic moment per atom ($\overline{\mu} = \sum_i \mu_i/N$) of the Rh_N clusters are obtained at the end of the self-consistent cycle. For a more detailed discussion of the model the reader may consult references [9,10].

3 Results

The initial cluster geometries, *i.e.*, before any hydrostatic deformation was applied, were obtained from an evolutionary search algorithm [genetic algorithm (GA) for short] applied to a many-body Gupta potential in the second moment approximation with a Born-Mayer term to describe the repulsive part [33,40]. Here, for the sake of simplicity, we restrict ourselves to the case of structures characterized by symmetric closed shells, that is, tetrahedron and rhombus for $N = 4$; hexahedron and square pyramid for $N = 5$; octahedron for $N = 6$; decahedron for $N = 7$; icosahedron for $N = 13$; double-icosahedron for $N = 19$; $N = 23$ and 26 poly-icosahedra and $N = 38$ cubo-octahedral (fcc-fragment). Starting from these geometries, a uniform expansion (compression) up to $\pm 10\%$ in bond length has been performed. This process preserves the cluster's point group symmetry and is called "an hydrostatic deformation". An expansion factor of one ($f = 1$) corresponds to the structure coming out from the geometry optimization. The average bond distance (ABD) of the $f = 1$ structure is indicated in every case. In order to assess our results, we have performed additional FP-DFT calculations for small (selected) clusters using Gaussian98 [41,42].

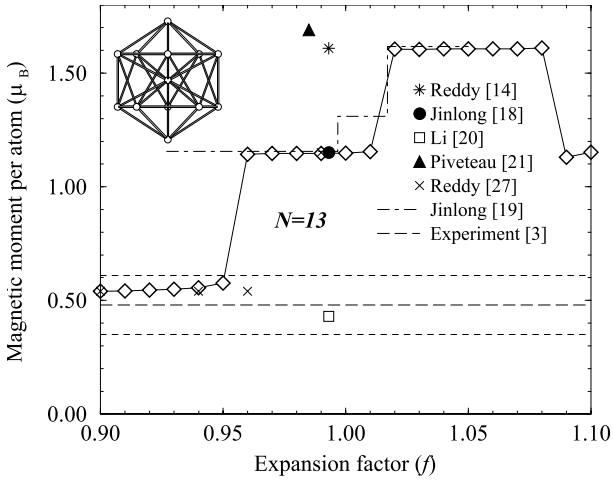

Fig. 1. Comparison of our results (represented by —◇—) with the different theoretical and experimental values available in the literature. The horizontal long-dashed line corresponds to the experimental value and the two parallel dashed lines correspond to the error bars [3]. Horizontal lines are used due to the fact that geometrical structures and bond lengths are unknown.

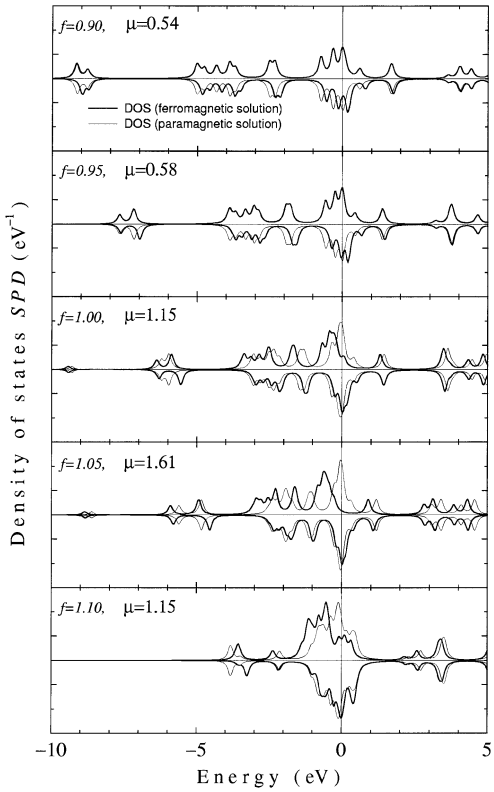

Fig. 2. Magnetic and paramagnetic *spd* density of states as a function of the expansion factor f. The Fermi level is fixed such that corresponds to $E = 0$ eV.

Our results show two different magnetic behaviors as a function of the expansion factor f depending on the cluster size N. One can distinguish two regions: $N \leq 13$ and $N > 13$. In general, for $N \leq 13$ the magnetic moment as a function of f displays a steplike dependence with an increasing number of steps depending on the number of atoms or on the local symmetry, whereas for $N > 13$ a smooth dependence of the magnetic moment as a function of the f factor is observed. This steplike behavior in the case of $N \leq 13$ is consistent with the fact that a system with few atoms (therefore few electrons) has fewer magnetic solutions associated to unpaired electrons. The magnetic solutions change abruptly when the expansion factor reaches a critical value.

Let us discuss in detail the case of Rh_{13} (see Fig. 1), as a typical cluster that exhibits a steplike behavior of the magnetic moment. We have chosen this cluster because it has been extensively studied in literature. Jinlong *et al.* [19] and Reddy *et al.* [27] have also found a steplike behavior of the magnetic moment *vs.* interatomic distance, in both cases using a DFT approach, although their results differ in the location of the steps. We obtain partial agreement with both DFT calculations. We have found, however, in addition, an unexpected magnetic behavior for $f \approx 1.08$, that corresponds to an expansion not considered in both DFT studies. We will come later to this aspect.

Within an atomic-like description, the occurrence of the magnetic solutions associated to the increasing steps is explained in terms of the HOMO-LUMO gap. As the expansion factor and interatomic distance increases, the LUMO states come closer to the HOMO states. Thus it is energetically favorable to transfer electrons from the minority to the majority states so that the gain in exchange energy is higher than the kinetic energy needed to occupy the high-energy states. The cluster is therefore expected to suddenly change to another spin multiplicity corresponding to the higher magnetic moment of the next step. Figure 2 displays the spin-polarized, together with, the paramagnetic DOS for Rh_{13} for various values of the expansion factor f. The states around the Fermi level have a *d*-character, while the *sp*-*d* hybrids are located far from the center of gravity of the DOS, as usual in TM systems. The DOS shows the narrowing and the increase of the splitting as going from one step to the next. According to the Stoner criterion, tendency to ferromagnetism increases together with the value of the DOS at the Fermi level. In the paramagnetic DOS one can observe a sharp peak close to the Fermi level and a qualitative correlation between the value of the DOS at the Fermi level and the magnetic moment as a function of the expansion factor.

As indicated in the Introduction, it is known that rhodium clusters exhibit anomalous magnetic behavior. Our results give further support to this fact since large deformations lead to a lowering of the magnetic moment. This is the case of Rh_{13} for f close to 1.10. Taking into account the *d*-electronic occupation in the system we can explain the apparently anomalous decrease of the magnetic moment in Rh_{13} as changing f from 1.05 to 1.10. One can observe that for $f = 1.05$, the first derivative of the paramagnetic DOS is negative (see Fig. 3), that is, the sharp peak has its maximum in the occupied region. Since rhodium has a more than half-filled *d* band, it is expected

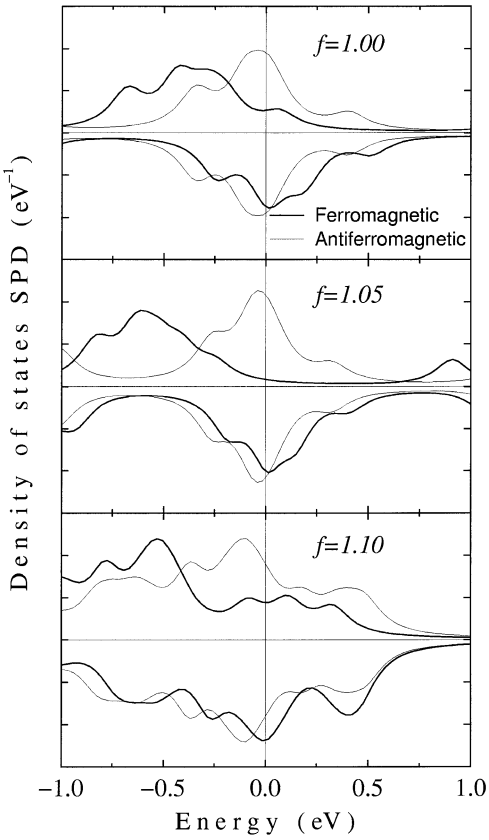

Fig. 3. Detailed dependence of the magnetic and paramagnetic *spd* DOS as a function of the expansion factor f for 1.00, 1.05, 1.10, to illustrate the slope of the DOS near the Fermi level.

that the narrowing of the DOS (associated to the expansion of the system) leads to a shift of the peak to lower energies and consequently to a decrease of the value of the DOS at the Fermi level. This is what we have obtained as going from $f = 1.05$ to 1.10 and, therefore, the reason of the decrease of the magnetic moment. One may wonder why this is not the case as going from $f = 1.00$ to 1.05. In such a case, however, the maximum of the peak is less pronounced, being the first derivative of the DOS at $E_{\rm F}$ being lower than before. We conclude that it is necessary to analyze the situation in detail and that it is not enough, at least in the case of rhodium, to discuss only in terms of simple geometrical parameters like the interatomic distances and coordination.

In the case of clusters with $N > 13$ the number of possible magnetic solutions associated to different spin multiplicity increases. In terms of itinerant magnetism, it is reflected in a less structured DOS that leads to more progressive evolution of the magnetic moment *vs.* f. Instead of steps we obtain a smoother dependence, accompanied in most cases by oscillations. Let us now discuss the results for each cluster and compare them with the available results from other authors.

For $N = 4$ (tetrahedron, ABD = 2.62 Å) we obtained a nonmagnetic ground state in entire range of $f = 0.9$–1.1. Our results are in agreement with the different investigations that predict a zero magnetic moment for tetrahedra with expansion factors of 0.946 [18] and 0.954 [27]. Using our tight-binding ground-state geometry as the starting point, we performed a second geometry optimization using a first-principles density functional approach, obtaining a tetrahedral cluster with bond lengths that are 93% of the initial ones. For the second isomer of $N = 4$, a rhombus with an ABD of 2.60 Å, our results show a stepwise variation of the magnetic moment. For $f = 0.9$–1.05 the value magnetic moment is $0.5\mu_{\rm B}$, and it increases to $1.0\mu_{\rm B}$ for $f = 1.05$–1.1. Our magnetic moment agree with Chien's calculations [25] for a rhombus with an expansion factor of 0.923.

For $N = 5$ in the ground state (hexahedron, ABD = 2.63 Å), we have a flat dependence of the magnetic moment ($0.6\mu_{\rm B}$) in the entire range considered. Our results are in agreement with Jinlong calculations [18] for an hexahedron with an expansion factor of 0.958. The reoptimized geometry keep the hexahedral shape but with smaller size, $f = 0.965$. For the second isomer (square pyramid, ABD = 2.62 Å) in the range from 0.90 to 0.95 we have a smooth monotonous increase in the magnetic moment starting from $0.3\mu_{\rm B}$ at $f = 0.90$ and reaching $0.6\mu_{\rm B}$ at $f = 0.95$. For an expansion factor larger than $f = 0.95$ a level off behavior is observed with magnetic moment of $0.6\mu_{\rm B}$. Other calculations in the literature give much larger magnetic moments $1.0\mu_{\rm B}$ and $1.4\mu_{\rm B}$ for square pyramids with expansion factors of 0.965 and 0.97, respectively [25,27]. In this case, the FP-DFT geometry reoptimization leads to a cluster size corresponding to an expansion factor of 0.965 and magnetic moment of $0.6\mu_{\rm B}$.

For $N = 6$ (an octahedron with ABD = 2.63 Å) displays an steplike function with three different values for the magnetic moment (see upper panel of Fig. 4): the magnetic moment jumps from zero in the range $f = 0.9$–0.96 to $1.0\mu_{\rm B}$ for $f = 0.97$–1.04, and then it jumps again to $1.33\mu_{\rm B}$ for $f = 1.05$–1.1. Jinlong [18], Reddy [27], and Li [20] predict zero magnetic moment for $f = 0.966$, 0.981, and 1.0, respectively, whereas our result predicts zero magnetic moment for f in the range 0.90 to 0.96. Our calculations agree with the results of both Chien [25] and Zhang [22] for a cluster size with an expansion factor of 0.989. Our FP-DFT geometry reoptimization predicts once again the octahedral arrangement but with smaller sizes $f = 0.938$ for the SVWN and $f = 0.947$ for the PW91-PW91 exchange-correlation parametrization. In both cases the magnetic moment is zero, in agreement with Jinlong's calculation [18] for an octahedron of an equivalent expansion factor of 0.966 and zero magnetic moment. As a general result, the reoptimization of the geometrical structure shows that the GA leads to the right geometry. However, the out coming cluster size is slightly larger than the ones proposed by the *ab initio* calculations in about 5%. Differences between the semiempirical bond length calculations and the *ab initio* method are also reported by Reddy [27].

For $N = 7$ we obtained a the decahedron (ABD = 2.65 Å) as the ground state. We observe a steplike function with two levels or values of the magnetic moment: $0.13\mu_{\rm B}$

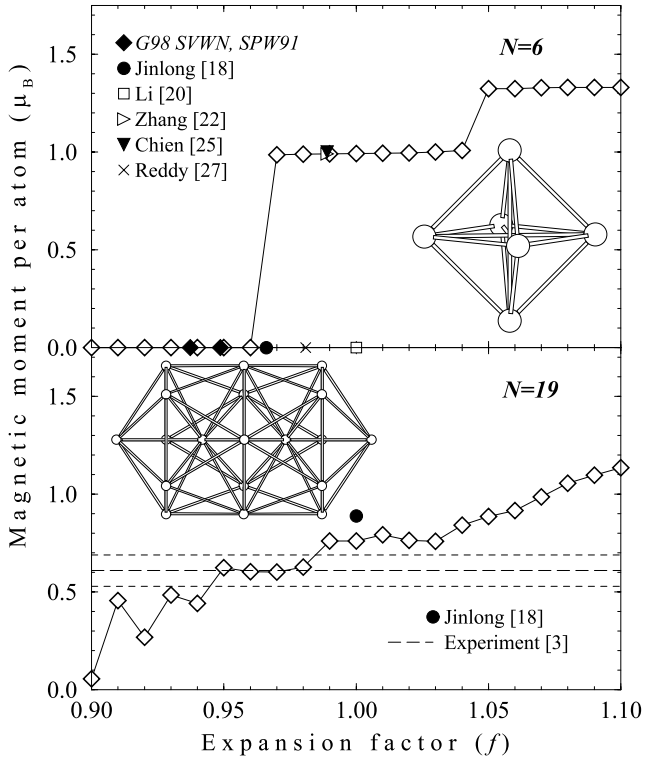

Fig. 4. Comparison of our results (represented by —◇—) with the different theoretical and experimental values available in the literature. The horizontal long-dashed line corresponds to the experimental value and the two parallel dashed lines correspond to the error bars [3]. Upper part corresponds to $N = 6$ and the lower part to $N = 19$.

from $f = 0.9$ to 1.07 and $0.73\mu_B$ from $f = 1.08$ to 1.1. Jinlong [18] and Reddy [27] predict smaller clusters than the GA with $f = 0.974$ and 0.985, respectively and the magnetic moment ($1.28\mu_B$) is larger than ours.

For $N = 13$ we have an icosahedral cluster (ABD = 2.68 Å). As Rh_{13} is expanded from $f = 0.9$, the magnetic moment increases in a steplike fashion showing three different values in the magnetic moment up to an expansion factor of about 1.08. Then it starts decreasing in contrast to the general rule, as discussed previously. We have included for comparison the results available in the literature. It is interesting to note that although all the calculations give nearly the same volume, there is a large dispersion in the values of the magnetic moments, the lowest being that reported by Li [20] with $0.43\mu_B$ for an icosahedral arrangement with an $f = 0.993$ and the largest $1.69\mu_B$ for $f = 0.985$ by Piveteau [21] There are in the literature two systematic studies of the dependence of the magnetic moment with the bond length one by Jinlong [19] and the other one by Reddy [27]. It is important to note that Jinlong's dependence presents a step value of $1.31\mu_B$ not previous reported in the literature. In view of our results, the differences in the magnetic moment obtained with the different methods are not associated with the different interatomic distances since in the range of the compression factor $f = 0.98$ to 1.01, corresponding to the geometrical results of other calculations, we do not obtain significant changes of the magnetic moment. When we compare with the experimental results represented by a long-dashed horizontal line (the short-dashed lines represent the experimental error bars), our results suggest that if the icosahedron is the right geometry, the experimental cluster size should be in the range of 0.9 to 0.95 of the expansion factor.

For the first isomer of $N = 19$ we obtained a double icosahedron (ABD = 2.69 Å) as the ground state structure. For the magnetic moment we obtain an increasing function of the expansion factor with some oscillations in the range of $f = 0.9$ to 0.95. Beyond this range we have an smooth increasing dependence, as it is shown in the lower panel of Figure 4. Jinlong's calculations [18] give larger values for the magnetic moment ($0.89\mu_B$ for $f = 1$). Concerning the experimental results, if we assume that the geometry is the double icosahedron, the best theoretical fit to the experimental values corresponds to expansion values in the range $f = 0.95$ to 0.98.

For $N = 23$ and $N = 26$, we have poly-icosahedral closed-packed clusters (ABD = 2.71 and 2.72 Å, respectively). In general we have complex dependences with oscillations for small expansion factors and a steplike increase in the magnetic moment for $f > 1.0$, as it is illustrated in the upper and middle panels of the Figure 5. If we assume that the experimental geometry correspond to that of Figure 5, there is a wide range of values that fit the experimental results, particularly those in the region of the small expansion values. However, in the case $N = 23$ there are some values outside of the error bars. In the case of $N = 26$, the range that fits best the experimental results is from $f = 0.9$ to 1.04 due to the small amplitude of the oscillations. For $N = 23$ there exist calculations of bcc-fragments [24] considering only the d contribution and the magnetic moment ($0.35\mu_B$) is larger than ours for $f = 1.0$. This fact is consistent with the lower coordination presented in the bcc structures.

Finally, for the case of $N = 38$, the first isomer is a truncated cubo-octahedron cluster (fcc-fragment, ABD = 2.69 Å). The magnetic moment increases in general as the cluster size increases although some oscillations of small amplitude are present, as it is shown in Figure 5. We are not aware of any theoretical calculation available in the literature for the large clusters studied in the present work ($N = 23$, 26, 38). If we assume that the experimental structure is the cubo-octahedral the best fit is in the range of $f = 0.90$ to 0.96.

In general, the reported results support the fact that for the best fit to the experiments, the real structures should be a little compressed with respect to those reported in the literature, since expansion factors slightly lower than 1 have to be considered in most cases.

4 Summary and conclusions

We have studied the magnetic properties of small Rh clusters as a function of a uniform expansion in the bond length. The studied geometries are those reported in the

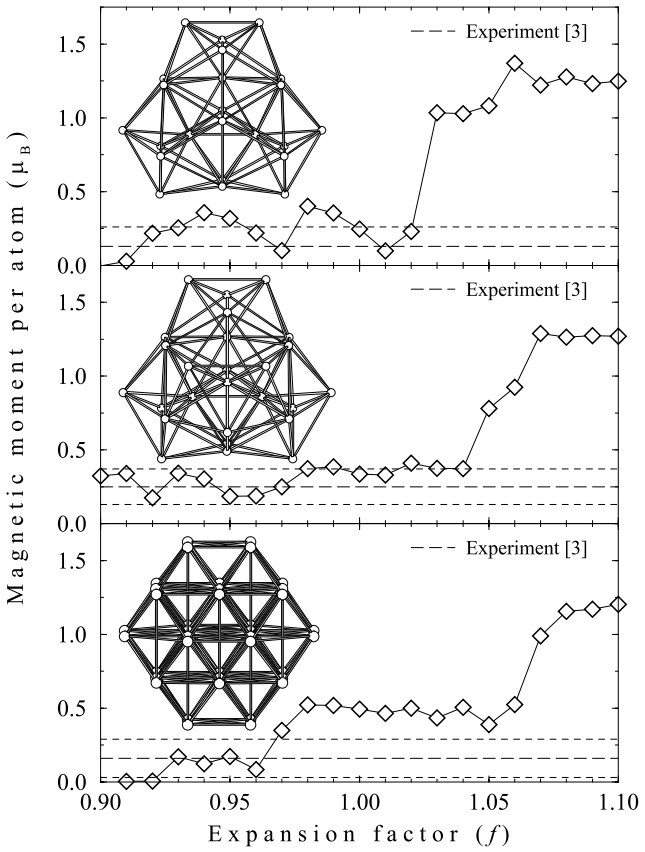

Fig. 5. Comparison of our results (represented by —◇—) with the experimental values available in the literature. The horizontal long-dashed line corresponds to the experimental value and the two parallel dashed lines correspond to the error bars [3]. Upper part corresponds to $N = 23$, the middle one to $N = 26$ and the lower part to $N = 38$.

literature obtained using the genetic algorithm [33]. The spin-polarized electronic structure of the clusters was calculated using a Hubbard type Hamiltonian for the $4d, 5s$ and $5p$ valence electrons within the unrestricted Hartree-Fock approximation [9,10].

We conclude that for a fixed geometry the magnetic moment is very sensitive to bond-length variations. Although symmetry and geometry play an important role in the magnetism of Rh clusters (as in other TMs clusters), here it is not always possible to rationalize the magnetic behavior in terms of simple geometrical parameters, as it is the case in $3d$ clusters [9].

Our study shows that many of the results published in the literature are consistent with our calculations considering the fact that reported bond-length values are slightly different. Consequently, different magnetic moment is expected. Not all the cases can be explain under this simple scheme due to the fact that the magnetic moment is also very sensitive to the type of calculations and approximations used.

As a general result, we find two size ranges, $N \leq 13$ and $N > 13$, according to the magnetic moment dependence with the expansion factor f. In the smaller sizes ($N \leq 13$) the magnetic moment displays a stepwise behavior as a function of the interatomic separation. For $N > 13$ we obtain a smoother dependence, accompanied generally by oscillations. The complex dependence with the expansion factor in Rh clusters characterized sometimes by anomalous magnetic behavior is related with the electron population in the neighborhood of the Fermi level. A detailed analysis has to be carried out in order to understand such subtle and complex behavior.

In general, for the best fit to the experiments, the real structure should be a little compressed with respect to those reported in the literature, since expansion factors slightly lower than 1 have to be considered in most cases. The present work is only a first step towards the understanding of the magnetism of low-dimensional rhodium systems. Further work is necessary, not only from the theoretical side, but also from the experimental one. It is important to point out that there exist only one experimental study on Rh clusters performed in 1993, up to our knowledge [3]. From the theoretical point of view, it would be pertinent to investigate the effect of possible Jahn-Teller distortions, particularly in the case of small size clusters where Jahn-Teller distortions are expected.

This work was partially funded by CONACyT (Mexico) under grants G-25851, J36909 and W-8001 (Millennium Initiative). Also to the CICyT, Spain, project PB98-0368-C02, and the Junta Castilla-León, Spain, grant VA 70/99. FAG acknowledges the partial support of FONDECyT, Chile, trough grants 1010511 and 7010511. Finally EOBR wishes to thank CONACyT for the financial support through the Ph.D. Fellowship Program.

References

1. D.M. Cox *et al.*, Phys. Rev. B **32**, 7290 (1985)
2. L.M. Falicov *et al.*, J. Mater. Res. **5**, 1299 (1990), and references therein
3. A.J. Cox, J.G. Louderback, L.A. Bloomfield, Phys. Rev. Lett. **71**, 923 (1993); A.J. Cox, J.G. Louderback, S.E. Apsel, L.A. Bloomfield, Phys. Rev. B **49**, 12295 (1994)
4. W.A. de Heer, P. Milani, A. Châtelain, Phys. Rev. Lett. **65**, 488 (1990)
5. J.P. Bucher, D.C. Douglass, L.A. Bloomfield, Phys. Rev. Lett. **66**, 3052 (1991)
6. D.C. Douglass, A.J. Cox, J.P. Bucher, L.A. Bloomfield, Phys. Rev. B **47**, 12874 (1993)
7. I.M. Billas, J.A. Becker, A. Châtelain, W.A. de Heer, Phys. Rev. Lett. **71**, 4067 (1993)
8. I.M. Billas, A. Châtelain, W.A. de Heer, Science **265**, 1682 (1994)
9. F. Aguilera-Granja *et al.*, Phys. Rev. B **57**, 12469 (1998)
10. J.L. Rodríguez-López, F. Aguilera-Granja, K. Michaelian, A. Vega, to be published
11. A.N. Andriotis, M. Menon, Phys. Rev. B **59**, 15942 (1999)
12. F.A. Reuse, S.N. Khanna, S. Bernel, Phys. Rev. B **52**, 11650 (1995); F.A. Reuse, S.N. Khanna, Chem. Phys. Lett. **234**, 77 (1995)
13. R. Galicia, Rev. Mex. Fís. **32**, 51 (1985)

14. B.V. Reddy, S.N. Khanna, B.I. Dunlap, Phys. Rev. Lett. **70**, 3323 (1993)
15. K. Lee, Z. Phys. D **40**, 164 (1997)
16. R. Guirado-López, D. Spanjaard, M.C. Desjonquères, F. Aguilera-Granja, J. Magn. Magn. Mater. **186**, 214 (1998)
17. J. Guevara, A.M. Llois, F. Aguilera-Granja, J.M. Montejano-Carrizales, Solid State Commun. **111**, 335 (1999)
18. Y. Jinlong, F. Toigo, W. Kelin, Phys. Rev. B **50**, 7915 (1994)
19. Y. Jinlong, F. Toigo, W. Kelin, Z. Manhong, Phys. Rev. B **50**, 7173 (1994)
20. Z.Q. Li, J.Z. Yu, K. Ohno, Y. Kawazoe, J. Phys. Cond. Matt. **7**, 47 (1995)
21. B. Piveteau, M.C. Desjonquères, A.M. Olés, D. Spanjaard, Phys. Rev. B **53**, 9251 (1996)
22. G.W. Zhang, Y.P. Feng, C.K. Ong, Phys. Rev. B **54**, 17208 (1996)
23. S.K. Nayak *et al.*, Phys. Rev. B **56**, 8849 (1997)
24. P. Villaseñor-González, J. Dorantes-Dávila, H. Dreyssé, G.M. Pastor, Phys. Rev. B **55**, 15084 (1997)
25. C-H. Chien, E. Blaisten-Barojas, M.R. Pederson, Phys. Rev. A **58**, 2196 (1998)
26. R. Guirado-López, D. Spanjaard, M.C. Desjonquères, Phys. Rev. B **57**, 6305 (1998)
27. B.V. Reddy *et al.*, Phys. Rev. B **59**, 5214 (1999)
28. R. Pfandzelter, G. Steierl, C. Rau, Phys. Rev. Lett. **74**, 3467 (1996)
29. A. Goldoni *et al.*, Phys. Rev. Lett. **82**, 3156 (1999)
30. E.K. Parks, G.C. Nieman, K.P. Kerns, S.J. Riley, J. Chem. Phys. **107**, 1861 (1997)
31. E.K. Parks, B.J. Winter, T.D. Klots, S.J. Riley, J. Chem. Phys. **96**, 8267 (1992); *ibid.* **99**, 5831 (1993); M. Pellarin *et al.*, Chem. Phys. Lett. **217**, 349 (1994)
32. P. Balone, R.O. Jones, Chem. Phys. Lett. **233**, 632 (1995)
33. F. Aguilera-Granja, J.L. Rodríguez-López, K. Michaelian, E.O. Berlanga-Ramírez, A. Vega, Phys. Rev. B **66**, 224410 (2002)
34. J.P.K. Doye, D.J. Wales, New J. Chem. **22**, 733 (1998)
35. K. Michaelian, Chem. Phys. Lett. **293**, 202 (1998)
36. K. Michaelian, Am. J. Phys. **66**, 231 (1998)
37. D.A. Papaconstantopoulos, *Handbook of the Band Structure of Elemental Solids* (Plenum, New York, 1996)
38. We have selected the icosahedral geometry because is a representative structure for the 13-atom cluster, as shown by a number of calculations
39. R. Haydock, *Solid State Physics*, edited by E. Ehrenreich, F. Seitz, D. Turnbull (Academic Press, London, 1980), Vol. 35, p. 215
40. For the technical details on GA as applied to cluster's geometry optimization, the interested reader is referred to reference [35,36] for a review
41. *Gaussian 98, Revision A.9*, M.J. Frisch, G.W. Trucks, H.B. Schlegel, G.E. Scuseria, M.A. Robb, J.R. Cheeseman, V.G. Zakrzewski, J.A. Montgomery, Jr., R.E. Stratmann, J.C. Burant, S. Dapprich, J.M. Millam, A.D. Daniels, K.N. Kudin, M.C. Strain, O. Farkas, J. Tomasi, V. Barone, M. Cossi, R. Cammi, B. Mennucci, C. Pomelli, C. Adamo, S. Clifford, J. Ochterski, G.A. Petersson, P.Y. Ayala, Q. Cui, K. Morokuma, D.K. Malick, A.D. Rabuck, K. Raghavachari, J.B. Foresman, J. Cioslowski, J.V. Ortiz, A.G. Baboul, B.B. Stefanov, G. Liu, A. Liashenko, P. Piskorz, I. Komaromi, R. Gomperts, R.L. Martin, D.J. Fox, T. Keith, M.A. Al-Laham, C.Y. Peng, A. Nanayakkara, M. Challacombe, P.M.W. Gill, B. Johnson, W. Chen, M.W. Wong, J.L. Andres, C. Gonzalez, M. Head-Gordon, E.S. Replogle, J.A. Pople (Gaussian Inc., Pittsburgh PA, 1998)
42. In our DFT calculations we used the LANL2DZ basis [43] and the SVWN method [44]. In the original minimization of the structures [33] spin-polarization was not considered
43. P.J. Hay, W.R. Wadt, J. Chem. Phys. **82**, 299 (1985)
44. S.H. Vosko, L. Wilk, M. Nusair, Can. J. Phys. **58**, 1200 (1980)